

Synthetic seismograms of the sea bottom under different streamer conditions

J. M. CARCIONE, G. PADOAN and F. CAVALLINI

Istituto Nazionale di Oceanografia e di Geofisica Sperimentale, Trieste, Italy

(Received November 26, 1998; accepted September 17, 1999)

Abstract. We obtain P-wave synthetic seismograms of the sea bottom for different streamer geometries, which may arise from several environmental conditions or vessel motions. The direct, reflected and receiver ghost are included in the modeling. The simulations illustrate the magnitude of the static corrections to be applied in off shore acquisition, due to the deviations from ideal streamer conditions.

1. Introduction

Static corrections for offshore seismic data may be necessary to account for the roughness and lateral velocity variations of the sea bottom, and due to deviations of the streamer line from a straight line. During operation, the streamer is subject to vessel motions as well as wave loads due to environmental factors (e.g., wave drift forces, currents and wind). In practice the problem is complex, since there is a different deformation of the streamer for each degree of freedom of the vessel (e.g., heave, surge and sway). The effects, due to the streamer location, are investigated by computing synthetic seismograms of the ocean bottom interface, assuming a rough air-water interface. For simplicity we assume two different deviations of the streamer line from a straight line: first an attenuating sinusoidal shape in the vertical plane with the nodes at the cable levelers and, second, a lateral bending from surge to sway, i.e., bending in the horizontal plane.

2. The wave equation and its solution

In the frequency domain, the acoustic wave equation for the pressure $p(\mathbf{x}; \omega)$ in water satisfies

$$(\nabla^2 + k^2)p(\mathbf{x}, \omega) = s(\mathbf{x}, \omega), \quad (1)$$

Corresponding author: J. M. Carcione; Istituto Nazionale di Oceanografia e di Geofisica Sperimentale, Borgo Grotta Gigante 42/c, 34010 Sgonico (TS), Italy; fax: +39 40 327521, e-mail: jcarcione@ogs.trieste.it

© 2000 OGS

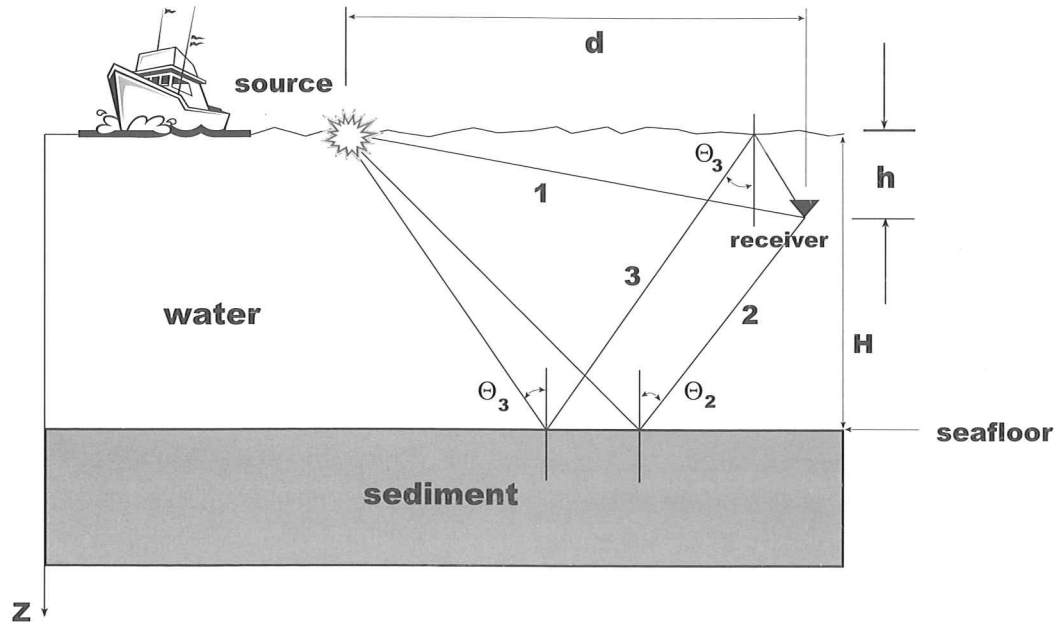


Fig. 1 - Raypaths from source to receiver for the direct wave (1), the reected wave (2) and the hydrophone ghost (3).

where \mathbf{x} is the position vector, ∇^2 is the Laplacian, c is the wave velocity, $k = \omega/c$ is the wave-number, and s is the source. We assume water to be a lossless medium. With proper boundary conditions the solution to Eq. (1) can be written as a volume integral

$$p(\mathbf{x}, \omega) = -\frac{1}{4\pi} \int g(\mathbf{x}, \mathbf{x}') s(\mathbf{x}', \omega) d\mathbf{x}', \quad (2)$$

where

$$g(\mathbf{x}, \mathbf{x}') = \exp(ikr)/r, \quad r = |\mathbf{x} - \mathbf{x}'| \quad (3)$$

is Green's function (e.g., Tolstoy and Clay, 1966).

Let us assume a monopole marine seismic source whose time history has a Fourier transform $F(\omega)$. Then,

$$s(\mathbf{x}', \omega) = \delta(\mathbf{x}' - \mathbf{x}_s) F(\omega), \quad (4)$$

where \mathbf{x}_s is the position of the source. Merging Eqs. (3) and (4) into Eq. (2) yields:

$$p(\mathbf{x}, \omega) = -\frac{1}{4\pi} F(\omega) \exp(ikr)/r, \quad (5)$$

where $r = |\mathbf{x} - \mathbf{x}_s|$ here.

Now consider the source-receiver configuration illustrated in Fig. 1, with the interface representing the sea bottom. Assume that the significant events are the direct wave (1), the reflected

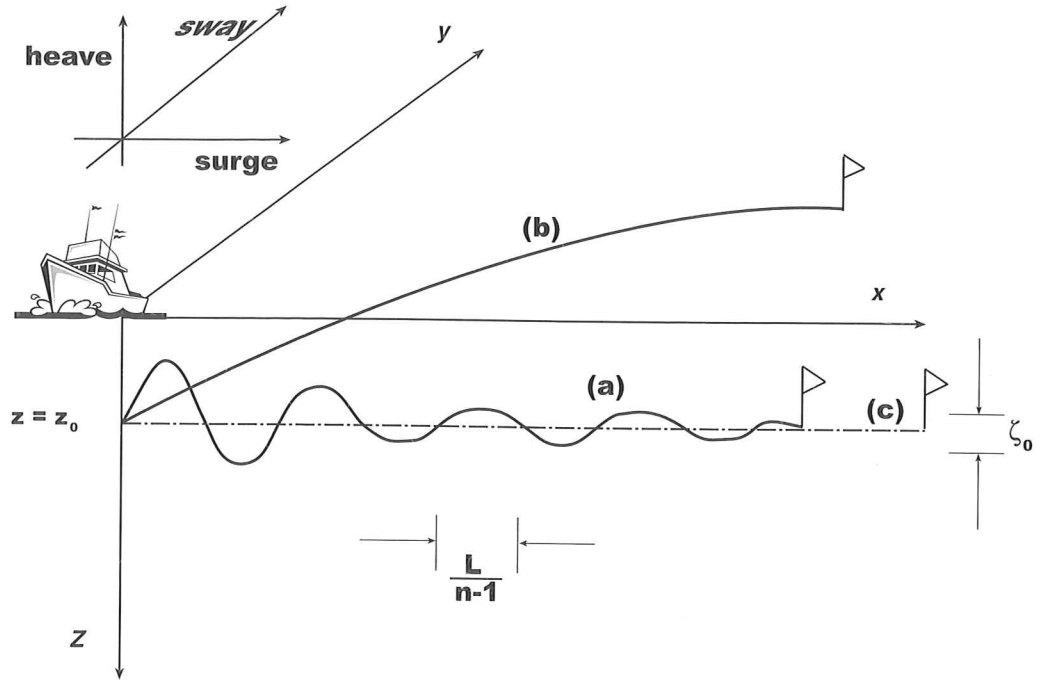


Fig. 2 - Simulated streamer geometries, where (a) is the attenuating sine function (13) and (b) corresponds to the cable shape (14). The streamer length is L , the distance between cable levelers is $L/(n-1)$ and the flag indicates the tail buoy. Finally, z_0 and ζ_0 are the mean depth of the streamer and the maximum amplitude in the vertical direction, respectively.

wave from the sea bottom (2) and the ghost at the hydrophone (3) (for simplicity, we neglect the source ghost and the roughness of the sea bottom). We can express the total field as

$$p(\mathbf{x}, \omega) = -\frac{1}{4\pi} F(\omega) \left[\frac{1}{r_1} \exp(ikr_1) + \frac{R(\theta_2)}{r_2} \exp(ikr_2) + A(\theta_3) \frac{R(\theta_3)}{r_3} \exp(ikr_3) \right], \quad (6)$$

where

$$\begin{aligned} r_1 &= \sqrt{h^2 + d^2} \quad (\text{direct wave}), \\ r_2 &= \sqrt{(2H-h)^2 + d^2} \quad (\text{reflected wave}), \\ r_3 &= \sqrt{(2H+h)^2 + d^2} \quad (\text{receiver ghost}). \end{aligned} \quad (7)$$

Assuming a pure acoustic sea-bottom sediment, the reflection coefficient is given by

$$R(\theta) = \frac{\rho V \cos \theta - \rho_w \text{p.v.} \sqrt{c^2 - V^2 \sin^2 \theta}}{\rho V \cos \theta + \rho_w \text{p.v.} \sqrt{c^2 - V^2 \sin^2 \theta}} \quad (8)$$

where p.v. denotes the principal value, ρ_w is the water density, ρ is the sediment density and V is the complex velocity of the sediment, whose anelastic properties are modeled by a continuous distribution of relaxation times (Ben-Menahem and Singh, 1981). Using this model, the complex

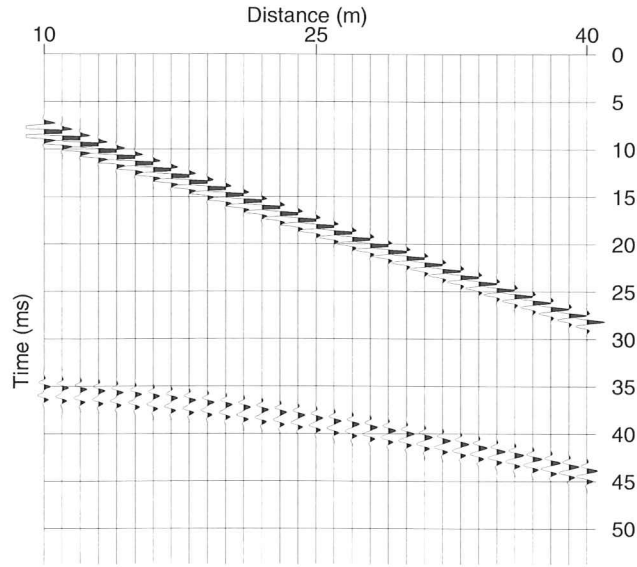


Fig. 3 - Synthetic seismograms corresponding to ideal streamer conditions (i.e., straight line).

velocity is obtained from the following equation:

$$V^2 = V_0^2 \left[1 + \frac{2}{\pi Q} \ln \left(\frac{1 + i\omega\tau_2}{1 + i\omega\tau_1} \right) \right]^{-1}, \quad (9)$$

where V_0 is the relaxed velocity, ω is the angular frequency, τ_1 and τ_2 are time constants, with $\tau_2 < \tau_1$, and Q denotes the value of the quality factor, which remains nearly constant over the selected frequency band.

The reflection coefficient at the surface is $A(\theta_3)$, for a smooth air-water surface we have $A = -1$, but the sea surface is generally a rough surface whose reflection coefficient can be expressed as

$$A(\theta_3, \omega) = -\exp\left(-\frac{2\omega^2}{c^2} \sigma^2 \cos^2 \theta_3\right), \quad (10)$$

where σ is the root-mean square (rms) amplitude of the surface roughness. Eq. (10) corresponds to a Gaussian surface. Because the sea surface is statistically modeled, the wavelet is the expected average of many wavelets at different sea heights. The rough surface acts as a Gaussian filter upon the reflected wave (see the discussion in Jovanovich et al., 1983).

The sea-bottom reflection angles for the first reflection and its ghost are, from Fig. 1,

$$\theta_2 = \arctan\left(\frac{d}{2H-h}\right), \quad \theta_3 = \arctan\left(\frac{d}{2H+h}\right). \quad (11)$$

Time-domain synthetic seismograms are obtained by performing an inverse Fourier trans-

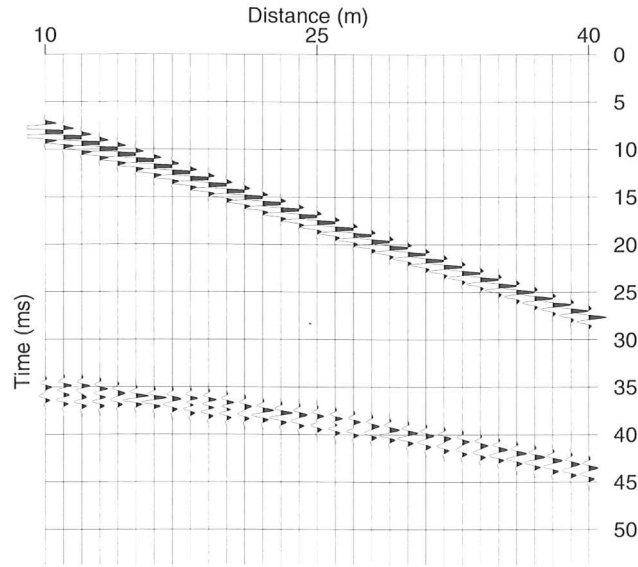


Fig. 4 - Synthetic seismograms corresponding to the combination of the sinusoidal line (13) and the cable shape (14).

form of $p(\omega)$.

3. Source function

To compute the seismograms we assume the following source time function

$$f(t) = \exp\left[-\frac{1}{2} f_c^2 (t - t_0)^2\right] \cos[\pi f_c (t - t_0)], \quad (12)$$

where f_c is the cut-off frequency and $t_0 = 3/f_c$. We do not claim that this “theoreticians’s wavelet” bears the signature of a standard marine seismic source; however, as we are investigating the effect of streamer shape and distortion, this simplified mathematical expression might suffice to illustrate the point. The time Fourier transform of the wavelet is

$$F(\omega) = \frac{\sqrt{2\pi}}{f_c} \exp\left[-\frac{1}{2} (\pi^2 + \omega^2 / f_c^2)\right] \cosh(\pi\omega / f_c) \exp(it_0\omega).$$

We point out that, for dissipative media, the frequency-domain Green's function has a singularity at zero frequency, which - a priori - seems troublesome. In our work we have overcome this problem by choosing a source whose Fourier transform has (for all practical purposes) a compact support not containing zero. In other words, the vanishing of the source at low frequencies “kills” the singularity of Green's function here. But, on a general scale, this question requires careful treatment.

Table 1 - Specification of main data.

<i>Medium properties</i>
Wave velocity of water, c : 1500 m/s. Density of water, ρ_w : 1028 kg/m ³ . Relaxed P-wave velocity of the sediment, V_0 : 2000 m/s. Sediment density, ρ : 2300 kg/m ³ . Upper relaxation time of the sediment, τ_1 : 1.6 s. Lower relaxation time of the sediment, τ_2 : 1.6×10^{-3} s. Quality factor of the sediment, Q : 20. Water column height, H : 25 m.
<i>Source characteristics</i>
Cut-off frequency, f_c : 2 kHz. Time delay, $t_0 = 3/f_c$: 1.5 ms.
<i>Sea surface</i>
Amplitude of the sea-surface roughness, σ : 0.5 m.
<i>Streamer data</i>
Nearest offset, d_0 : 10 m. Length, L : 30 m. Distance between hydrophone arrays, Δx : 1 m. Number of cable levelers, n : 31. Mean depth, z_0 : 0.75 m. Maximum amplitude in the vertical direction, ζ_0 : 0.5 m. Damping factor, a : $3/L$. Deviation angle at the vessel, ϕ_0 : 23°. Deviation angle at the tail buoy, ϕ_T : 8°.

4. Cable shape

Consider a streamer of length L and n cable levelers. Heave motions of the vessel, and attenuation with distance from the vessel, generate a streamer motion in the (x, z) vertical plane with $y = 0$, given by

$$z = z_0 + \zeta_0 \exp(-ax) \sin \left[\pi(n-1) \frac{x}{L} \right], \quad (13)$$

where z_0 is the mean depth of the streamer and ζ_0 is the maximum amplitude in the vertical direction (see Fig. 2) and a is the damping factor. The distance between cable levelers is $L/(n-1)$.

A straight streamer bending from surge to sway (due to the wind or to oceanic currents) in the horizontal (x, y) -plane with $z = z_0$, has the following cable curve shape (Krail and Brysk, 1989):

Table 2 - Position of the tail buoy.

Cable shape	x_T (m)	y_T (m)	z_T (m)	r_T (m)
Straight line	40	0	0.7	40.006
Sine	39.47	0	0.717	39.476
Eq. (14)	39.15	6.75	0.7	39.734
sine + Eq. (14)	38.661	6.685	0.73	39.241

$$y = BL \ln \left[\frac{1 + \cos \phi_0}{1 - A + \sqrt{\cos^2 \phi_0 - 2A + A^2}} \right], \quad (14)$$

where

$$A = \frac{x \sin \phi_0}{BL}, \quad B = \frac{1}{\cot \phi_0 - \cot \phi_T}. \quad (15)$$

Here ϕ_0 is the angle between the vessel's course and the streamer at the vessel location, and ϕ_T is the angle between the vessel's course and the streamer at the tail buoy.

5. Examples

Let us consider the case of very high resolution marine data (Wardell et al., 1999). The data given in Table 1 is representative of this situation. Fig. 3 shows the synthetic seismograms for ideal streamer conditions (i.e., streamer lying in a straight line). The first event is the direct wave and the second event is formed by the interfering hyperbolas corresponding to the reflected wave and ghost. The seismogram corresponding to the combination of the attenuating sinusoidal function (13) and the lateral bending (14) is illustrated in Fig. 4, where the wavy behavior due to the sinusoidal shape of the streamer can be observed at the near offsets. A closed comparison can be appreciated in Fig. 5, where 5a and 5b correspond to the near and far offsets of the straight line, respectively, and 5c and 5d correspond to the near and far offsets of the non-ideal conditions (Fig. 4). Maximum deviations are of the order of 0.5 ms at the near offsets and 0.25 ms at the far offsets, which are comparable to the residuals obtained by Wardell et al. (1999). In Fig. 5d the reflections arrive earlier than the reflections of Fig. 5c, since the tail buoy is closer to the source when the streamer has a sinusoidal shape. The position of the tail buoy (corresponding to the last trace) for the different cable shapes is given in Table 2. The deviations due to the sine function are larger than the deviations due to the lateral bending.

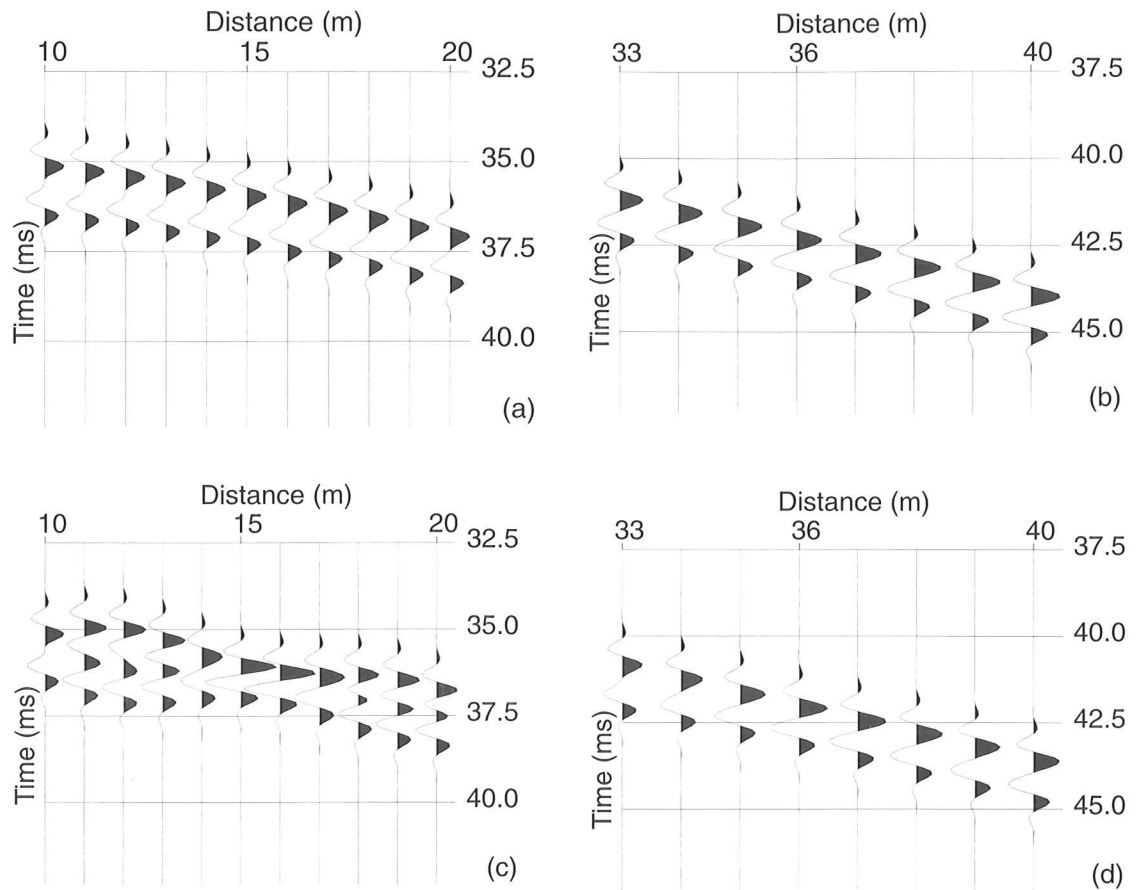


Fig. 5 - Blow-up of near- and far-offset traces for the straight line (a and b, respectively), and near- and far-offset traces for the non-ideal streamer shape (c and d, respectively).

6. Conclusions

A modeling tool describing the effects of the streamer conditions on the sea-bottom seismic response has been developed. We considered the direct wave, the reflected wave and the hydrophone ghost, assuming a rough sea surface. The modeling is suitable for analysis of static corrections arising from different streamer positions with respect to the ideal streamer configuration (i.e., a straight line). In this work, we obtained (besides the ideal case) the synthetic seismograms from the combination of an attenuating sinusoidal geometry in the vertical plane along the surge direction, and a lateral bending towards the sway direction, confined to the horizontal plane. With our choice of parameters, the main differences are between traces corresponding to wavy or non wavy geometries.

Acknowledgments. This work was financed, in part, by the European Union under the MAST project VHR3D "Very high-resolution marine 3D seismic method for detailed site investigation", Contract Nr. MAS3-CT97-0121. Helpful discussions with N.Wardell are gratefully acknowledged.

References

- Ben-Menahem A. and Singh S. G.; 1981: *Seismic waves and sources*. Springer Verlag, Berlin.
- Jovanovich D. B., Sumner R. D. and Akins-Easterlin S. L.; 1983: *Ghosting and marine signature deconvolution: A prerequisite for detailed seismic interpretation*. *Geophysics*, **48**, 1468-1485.
- Krail P. M. and Brysk H.; 1989: *The shape of marine streamer in a cross current*. *Geophysics*, **54**, 302-308.
- Tolstoy I. and Clay C. S.; 1966: *Ocean acoustics: Theory and Experiment*. In: Underwater sound. New York, McGraw-Hill.
- Wardell N., Diviaco P., Sinceri R. and Rossi G.; 1999: *Determination of static corrections on very high resolution marine data*. 61st Ann. Internat. Mtg. Europ. Assoc. Expl. Geophys., Expanded Abstracts, P010.